Journal of Photochemistry and Photobiology A: Chemistry 200 (2008) 126–140

Contents lists available at ScienceDirect

Journal of Photochemistry and Photobiology A: Chemistry

journal homepage: www.elsevier.com/locate/jphotochem

Using hyperbranched macromers as crosslinkers of methacrylic networks prepared by photopolymerization

Sara Pedrón, Paula Bosch, Carmen Peinado*

Instituto de Ciencia y Tecnología de Polímeros, CSIC, Juan de la Cierva 3, 28006 Madrid, Spain

ARTICLE INFO

Article history:
Received 14 May 2008
Received in revised form 1 July 2008
Accepted 2 July 2008
Available online 11 July 2008

Keywords:
Hyperbranched macromers
Photopolymerization
Fluorescence
Networks
Self-assembly

ABSTRACT

Hyperbranched polymers were modified with terminal methacryloyl groups to be used as crosslinkers. The photoinitiated polymerization of several methacrylic monomers was examined in the presence of the hyperbranched macromers and *bis*-(2,4,6-trimethylbenzoyl)-phenylphosphine oxide (Irgacure 819®) as a photoinitiator, upon UV irradiation. The photopolymerization kinetics was systematically studied by fluorescence and photoDSC in real time and *in situ*. Six types of monofunctional methacrylic monomers, two types of difunctional methacrylic monomers and four types of (meth)acrylate-modified hyperbranched macromers with different structures were employed for series of photopolymerization reactions. The incorporation of the hyperbranched macromers allows to increase the conversion at gelation and thus, final conversion. This behaviour is dependent on monomer and macromer nature and has been explained as due to an increase of the free volume fraction and confirmed by fluorescence. The results indicate that H-bonding and π-stacking induce self-assembly of hyperbranched macromers leading to reaction induced phase separation at the highest concentration of hyperbranched macromer used.

Published by Elsevier B.V.

1. Introduction

Recently, society has become aware of the necessity to reduce or eliminate VOC (volatile organic compounds) emissions from coating applications. These reasons together with the growing demand for coatings in technologies and speciality applications have lead to chemists to look for alternatives to the traditional solvent-based coatings. Radiation-cured coatings, by means of EB (electron beam) or UV-light, have been developed and show the potential to replace conventional solvent-based systems that are ozone-depleting. UV-curing formulations include a photoinitiator in the formulation which under irradiation absorbs and converts UV–visible light into reactive intermediates, such as free radicals and radicals ions, and/or long lived intermediates, such as acids or bases, which initiate the photochemically driven polymerization that is normally completed in few seconds. Moreover, advantages of UV-curing technology such as costs saving, high manufacturing efficiency and environmental advantages are expected to be evaluated to replace conventional methods. Today, UV-curable material is not limited to the coating industry. It has found new applications in many other fields such as encapsulates for microelectronic device, silica-filler polymer composites, adhesives, sterolithography, dental restorative materials fillings, contact lens and optical discs [1].

The photoinitiated polymerization of (meth)acrylates is one of the most efficient processes for the rapid production of polymeric crosslinked materials with defined properties. However, methacrylates are subjected to several limitations including polymer shrinkage, oxygen inhibition and residual insaturation which have deleterious effects on polymer performance and lifetime. Several approaches have been developed to overcome these disadvantages. One of the most promising areas of research concerns the improvement of macromolecular properties by changes in the macromolecular architecture. Recently, Bowman and coworkers [2] have studied the photopolymerization kinetics of novel methacrylates which exhibit extensive polymerization in the dark compared to traditional acrylates and diacrylates. In the last decade hyperbranched polymers have been incorporated to the UV-curing technology for preparing thermoset coatings taking advantage of the high number of reactive end-groups and their particular topology.

Hyperbranched polymers (HBP) are a kind of dendritic polymers characterized by a tree-like architecture which confers them very different properties compared to their linear counterparts. It is generally accepted that the globular end-functionalized structure gives rise to a lower degree of entanglement (lower viscosity) and an enhancement of the end-chain effects. The structural control of hyperbranched polymers by increasing the degree of branching or

* Corresponding author.
E-mail address: cpeinado@ictp.csic.es (C. Peinado).

1010-6030/$ – see front matter. Published by Elsevier B.V.
doi:10.1016/j.jphotochem.2008.07.002

by modification of end-groups allows fine-tuning of the physical properties and thus, their applications.

HBPs have also been described in several applications, ranging from processing additives [3] to thermoset system components [4,5]. A wide range of waterborne hyperbranched polyurethane acrylates have been prepared for radiation curing of aqueous dispersions [6]. It has been shown that both hard and soft segments contents, in addition to the generation number of the hyperbranched polymer, can have significant effect on the physical and thermal properties of the aqueous dispersions [7]. Maruyama and co-workers [8] reported the synthesis of photocross-linkable hyperbranched poly(urethane)s containing both terminal methacryloyl groups and carboxyl groups. Photopatterning using the obtained hyperbranched polymers was achieved with good resolution. UV-curing behaviour of hyperbranched poly(siloxysilane)s containing vinyl, allyl and epoxy end-groups was extensively investigated in the presence of several photoaccelerators [9]. UV-curable acrylate modified hyperbranched polyisophthalester which exhibited high refractive index and good miscibility with comonomer, may meet the requirements of a prepolymer used for graded-index materials [10]. Dendritic hyperbranched polymers have been used as tougheners for epoxy resins [11] and polypropylene [12]. The high toughening capacity of HBP modifiers is suggested to be induced by the gradient properties obtained within the phase—separated particles. Epoxy functional hyperbranched polymers have been used to tailor interfacial properties of immiscible polymers [13]. The interfacial adhesion between fusion bonded plaques of PP and PA6 was strongly increased with the addition of the HBP grafted to PP compared to maleic anhydride grafted PP. It seems that hyperbranched polymers might be a good alternative to dendrimers inasmuch as the former can be produced on a large scale at a reasonable cost avoiding protection/deprotection steps needed in dendrimer synthesis. Recently, Peleshanko has reviewed recent developments in the field of HB molecules with emphasis in the growth of this research field in the last 5 years [14].

The potential of HBP on radiation curing has been put in evidence by a wide number of applications, some of them industrially developed. It is well-known that the structure of monomers influences the kinetics of the reaction and thus, the final properties of the material. In spite of this, there is a lack of detailed kinetic studies of the reaction of UV-curable HBP resins. Herein, we study the kinetics of photopolymerization of meth(acrylate)-modified hyperbranched macromers and methacrylic monomers by photocalorimetry and fluorescence.

Fluorescence has become an useful tool for monitoring dynamic processes in polymer research [15]. Both intrinsic and extrinsic fluorescence have been used to investigate polymer behaviour. Recently, our group has prepared fluorescent probes which are sensitive to rigidity/polarity of its microenvironment and used them for monitoring UV-curing of acrylic monomers and oligomers in homogeneous and microemulsion media [16]. This fluorescence-based method has revealed an interesting potential to study kinetics of photopolymerization as well as to study microstructure development during photopolymerization processes [17].

In order to give an overall view, we have systematically examined the influence of the presence of hyperbranched macromers (HBMm) in the kinetics of photopolymerization of acrylic monomers. Six types of monofunctional methacrylic monomers, two types of difunctional methacrylic monomers and four types of meth(acrylate)-modified hyperbranched macromers with different structures were employed for a series of photopolymerization reactions. The kinetic parameters were determined by DSC and compared with fluorescence data. Thermal stability of the HBMm crosslinked networks was measured by TGA and compression modulus was determined to assess mechanical resistance.

2. Experimental

2.1. Materials

Lauryl methacrylate (LMA), 2-hydroxyethyl methacrylate (HEMA), 2-ethylhexyl methacrylate (EHMA), butyl methacrylate (BMA), ethoxyethyl methacrylate (EEMA), octyl methacrylate (OMA), 1,6-hexanediol dimethacrylate (HDDMA) and poly(ethylenglycol) dimethacrylate (PEG-DMA, M_n = 550 Da) were purchased from Aldrich and were purified by distillation prior to use.

The HBPs used in this work are an aliphatic polyester Boltorn® H30 and polyesteramides Hybrane® P1000, H1500 and D2000. H30 has an ethoxylated pentaerythritol moiety as central core and 2,2-*bis*(methylol)propionic acid (*bis*-MPA) as dendritic units. This polymer has an average of three generations of MPA. Hybranes have di-2-propanolamine as end-group and differ in the building group. The building groups are cyclohexane dicarboxylic anhydride for H1500, 1-dodecenyl-ethyl dicarboxylic anhydride for D2000 and phtalic anhydride for P100. Hyperbranched polymer Boltorn® H30 was kindly provided by Perstorp, Sweden, and Hybrane® P1000, H1500 and D2000 were kindly supplied by DSM, The Netherlands. The idealized formulae of polyester H30 and polyesteramides P1000, H1500 and D2000 are shown in Figs. 1 and 2, respectively.

Photoinitiator *bis*-(2,4,6-trimethylbenzoyl)-phenylphosphine oxide (Irgacure 819®) was generously gifted by Ciba Specialty Chemicals, Basel, Switzerland, and used as received. The fluorescent probe, *N*,*N*-dimethyl-[4-(2-pyrazin-2-yl-vinyl)-phenyl]-amine (DMA-2,5), was synthesized as previously described [18]. Fig. 3 shows the structure of the probe and Scheme 1 the photofragmentation reaction of the photoinitiator upon irradiation.

2.2. Methacrylic functionalized hyperbranched polymers, HBMm

Modification of HBPs was carried out by esterification of hydroxyl groups with methacryloyl chloride. The corresponding hyperbranched polymer (1 mmol based on hydroxyl end-groups) and *N*,*N*-dimethylaminopyridine (0.05 mmol) were dissolved under nitrogen in dry dichloromethane (tetrahydrofuran for H30) and triethylamine (1.5 ml) in a reaction vessel. The flask was equipped with a drying tube and cooled on a water/ice-bath. Methacryloyl chloride (1.5 mmol), freshly distilled, diluted with dichloromethane was slowly added to the mixture and the solution was then left stirring at room temperature overnight. The solution was extracted twice with aqueous HCl (2%) and NaOH (2%) solutions, then dried over anhydrous $MgSO_4$, filtered, and finally evaporated, yielding a slight yellow viscous product.

The ^{1}H NMR integral of protons in the building blocks was used as reference for Hybranes and the integral of methyl protons for H30. The degree of substitution and the concentration of methacryic double bond of H30MA, P1000MA, H1500MA and D2000MA were determined by comparison of the reference integral signal with the ^{1}H NMR integral of the terminal methacrylate vinyl moiety. Data was supported by MALDI-TOF mass spectrometry. Table 1 contains data of synthesized materials.

2.3. Photopolymerizable samples

Methacrylic monomers were photopolymerized in the presence of different amounts of methacrylic end-capped hyperbranched polymers, HBMm. The photoinitiator (1%, w/w with respect to the

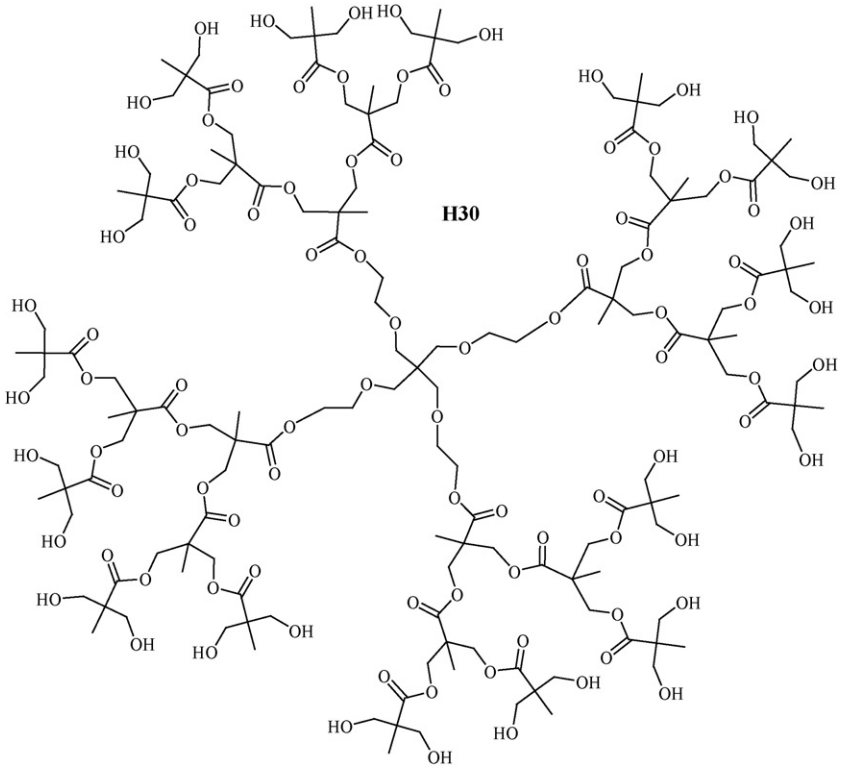

Fig. 1. Idealized structure of the hyperbranched polyester Boltorn® H30.

total weight of monomers) and the fluorescent probe (0.002%, w/w) were added to the samples.

2.4. Polymerization proceeding and analysis

A weighted amount of these samples were placed into an aluminium pan in the sample holder of a Shimadzu model DSC-50 and the temperature maintained at 10 °C using a cryostat Huber polystat CC1, to avoid monomer evaporation. Samples were irradiated under nitrogen *in situ* with a MACAM-Flexicure portable irradiation system provided with a Sylvania 400 W Hg medium-pressure lamp and twin quartz optical fiberguides. The simultaneous measuring of the fluorescence of the probe and the heat evolved in the polymerization was performed as previously described [16], using a DSC coupled to a spectrofluorimeter with a shortwave pass dichroic beamsplitter to separate irradiation and emission wavelengths, and recording a complete fluorescence spectrum each 14 s. The dichroic beamsplitter (Lambda) shows high transmission at long wavelengths ($\lambda > 400$ nm) and high reflectivity at shorter wavelengths ($\lambda < 100$ nm). Fluorescence is recorded by a PerkinElmer spectrofluorimeter LS-50. Incident light intensity was set constant for all runs at a value of 3 mW/cm^2.

Two parameters were used to show fluorescence changes, fluorescence intensity at maximum, and the first moment of fluorescence, $\langle\nu\rangle$. The first moment of fluorescence [19], $\langle\nu_F\rangle$, is given by the weighted average wavenumber in Eq. (1):

$$\langle\nu_F\rangle = \frac{\sum I_F(\nu)\,\nu}{\sum I_F(\nu)} \quad (1)$$

The heat flux was monitored as a function of time using the DSC under isothermal conditions and both polymerization rates and conversion were calculated as a function of time. A value of 54.7 kJ/mol was used as the theoretical heat evolved for polymerization of the methacrylic double bonds [20].

2.5. Characterization

The morphology of the photopolymerized networks was observed on a Philips XL30 environmental scanning electron microscopy (ESEM) provided of EDAX. Samples were frozen by immersing in liquid nitrogen, followed by mechanical fracturing.

Thermogravimetry (TGA) measurements were performed in a PerkinElmer thermobalance, model TGA 7. Measurements were carried out using 5 mg of sample and heated at a rate of 10 °C/min under nitrogen atmosphere. The onset degradation temperature (T_{on}) was defined as the initial temperature of degradation, corresponding to the intersection of tangent drawn at the intersection point of decomposition step with the horizontal zero-line of the TG curve. The glass transition temperatures were measured by a differential scanning calorimeter (Mettler823^e) at a heating rate of 5 °C/min, calibrated using standard procedures. T_g were determined as the midpoint of the transition.

Density measurements were performed using an AccuPyc 1330 Pycnometer with a 1 cm^3 sample insert. The pressures observed upon filling the sample chamber with the helium and then discharging it into a second empty chamber allows computation of the density of the sample.

2.6. Swelling of networks

In order to measure solvent absorption, the films prepared as described previously were transferred into glass vials and their initial weight (W_0) was recorded. Next, the vials were filled with 10 ml ethanol. The films were removed at regular time intervals, the surface solvent was gently removed by a paper towel, and then weighted until no further weight change was detected (W_t). The swelling ratio is defined as the percentage ratio between the weight at time t and its initial weight ($[W_t - W_0]/W_0 \times 100\%$).

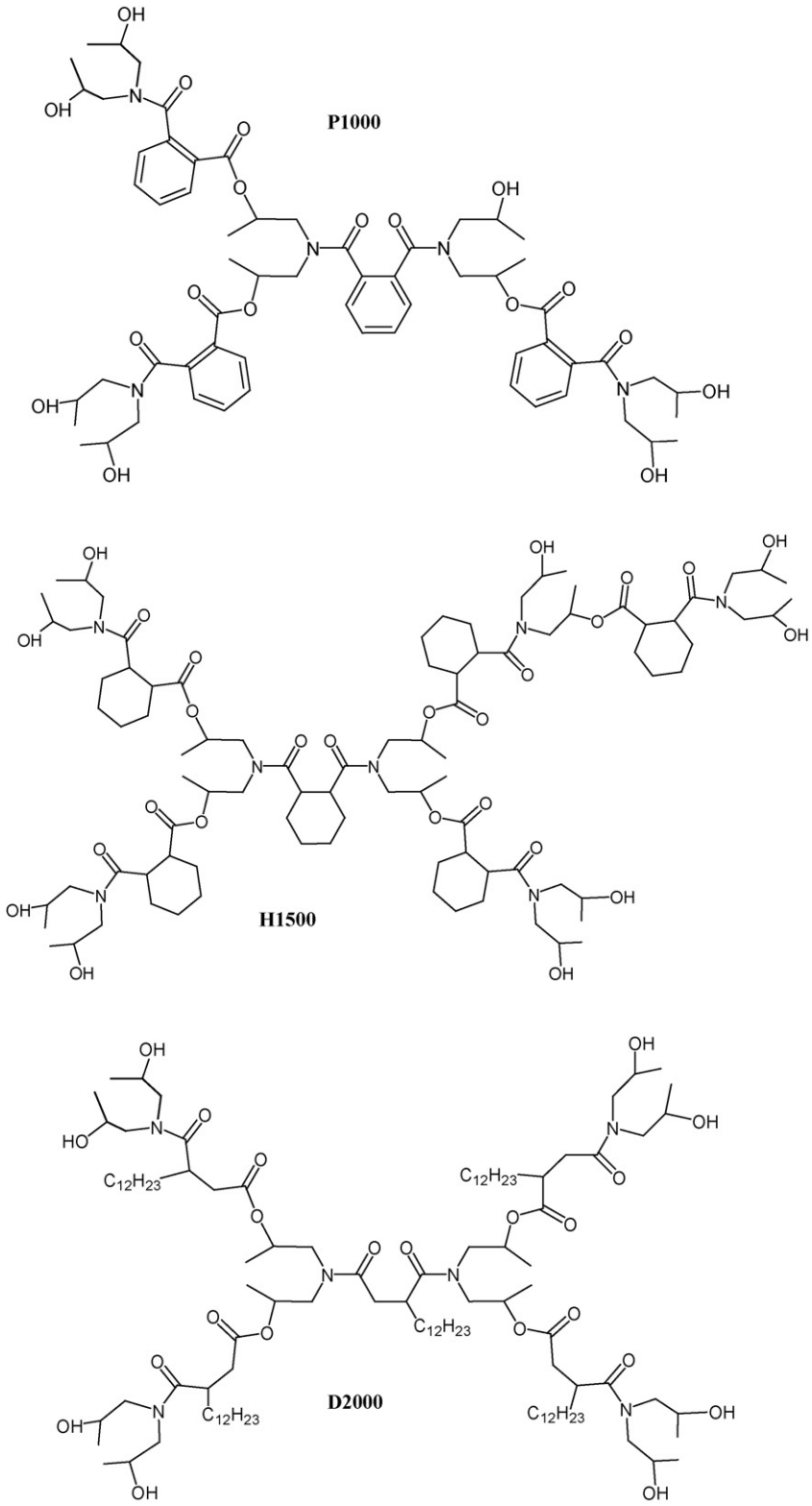

Fig. 2. Idealized structure of the hyperbranched polymers Hybranes® P1000, H1500 and D2000.

2.7. Compression testing

The compression modulus of the films was measured at room temperature using a mechanical testing machine MTS Bionix 100 (Model 810, MTS Systems Corp., Eden. Prairie, MN). After zeroing and taring the probe, sample disks of 4 mm diameter and 1.4 mm height were placed between parallel plates. Samples were compressed at a constant rate of 0.5 mm/s up to a strain of 20%. The resulting force (N) was measured as a function of the percent strain. The modulus (E) was calculated from the slope

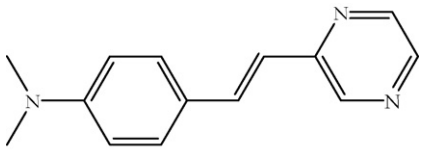

DMA-2,5

Fig. 3. Structure of the fluorescent probe.

of the best-fit line of the linear region of the stress–strain curve at less than 10% deformation of the various samples. Results are reported for data collected from at least three specimens for each material.

3. Results and discussion

The effect of the structure of multifunctional monomers on the polymerization rate and double bond conversion has been described in many reviews [21]. It was well established that higher degree of functionality (greater number of double bonds per monomer molecule) led to higher reaction rates, more rapid onset of gelation and vitrification and higher density of crosslinks. However, denser networks reduce the extent of double bond conversion, leaving a large portion of them unreacted (even 50%). The length of the chain connecting two unsaturations in the monomers also affects the reaction kinetics. In contrast to more typical multifunctional monomers, the hyperbranched macromers (HBMm) studied here have relatively high molecular weights and contain several pendant double bonds per chain (i.e., several crosslinking double bonds per molecule). Both of these features can significantly influence the overall polymerization behaviour and ultimate network structure. Therefore, the aim of this work was to study the kinetics of photocrosslinking reaction of acrylic monomers and HBMm by DSC and fluorescence measurements *in situ* and in real time.

3.1. Hyperbranched macromers

The hydroxyl end-groups of four hyperbranched polymers were functionalized with methacrylic reactive groups suitable for crosslinking. The functionalization was accomplished by a base catalyzed reaction of the hydroxyl end-groups with methacryloyl chloride (Scheme 2). The reaction was performed at low temperature under nitrogen atmosphere in order to prevent premature polymerization. Different fractions of non-reactive/reactive end-groups were achieved depending on HBMm structure and experimental conditions. NMR spectroscopy was used to quantify the conversion of end-groups. Hybrane-modified polymers have an average of 5–6 methacrylic functionalized end-groups whereas the polyester modified H30MA has an average of 16 methacrylic end-groups (from a total of 32 hydroxyl functionalities). Hydroxyl number, molecular weight and acrylic functionality are presented in Table 1.

Table 1
Hydroxyl number, molecular weight and acrylic functionality of the hyperbranched macromers

HBMm	Average number of hydroxyl end-groups[a]	M_n (g/mol)[a]	Average number of methacrylic end-groups[b]
H30MA	32	2300	16
P1000MA	7	1500	5
H1500MA	10	1500	6
D2000MA	8	2000	6

[a] Data provided by the manufacturer for the corresponding HBP precursors.
[b] Data obtained by ^{1}H NMR.

3.2. Kinetics of photopolymerization

The properties of a UV-cured film depend on the resin composition and also on the photopolymerization kinetics. Thus, the polymerization behaviour of methacrylic monomers in the presence of different amounts of HBMm was investigated using both DSC and fluorescence simultaneously in real time.

Fig. 4 shows the profile of polymerization rate as a function of conversion for several monomers in the presence of the hyperbranched macromer P1000MA, obtained from photoDSC measurement at 30 °C. Different behaviours may be distinguished depending on the monomer: (a) HEMA photopolymerization shows an unique peak, (b) LMA and BMA photopolymerization shows an unique peak in the absence of crosslinker and in the presence of a certain amount of P1000MA a shoulder is developed and (c) two peaks are observed for the rest of the formulations (EHMA and EEMA), both in the presence and in the absence of crosslinker.

An unique peak seems to be related to the photocuring of the monomers which show higher reactivity, such as HEMA. In polymer synthesis, it has been known for a long time that certain monomers such as methacrylate and acrylate derivatives exhibit an autocatalytic behaviour during the polymerization process. The modified autocatalytic model proposed by Kamal and Sorour [22] for isothermal cure of thermosetting resins is given below by the following equation:

$$\frac{dC}{dt} = kC^m(C_f - C)^n \quad (2)$$

where C is fractional conversion, k is the rate constant and m and n represent orders of initiation and propagation, respectively. The total order of the curing reactions, $m+n$, was assumed to be 2 for vinyl terminated resins [23]. This model was used to fit the experimental kinetic data obtained from photoDSC.

Fig. 5 plots the experimental and theoretical conversion rate versus fractional conversion for the UV-curing of HEMA in the presence of the hyperbranched macromer P1000MA (8%, w/w). Predicted rate constants and reaction orders are given in Table 2 for different amounts of P1000MA. The modified autocatalytic model shows a good fit to experimental data for all the formulations containing HEMA while the other studied monofunctional monomers follow an autocatalytic reaction only during the early time of reaction.

Fig. 4(c) and (d) shows different kinetic profiles with multiple peaks which are attributed to microgel formation [24]. The first

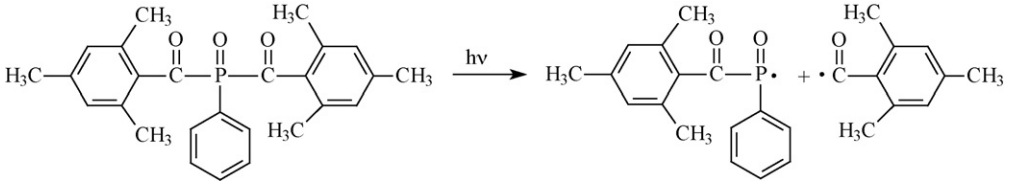

Scheme 1. Photofragmentation mechanism of the photoinitiator.

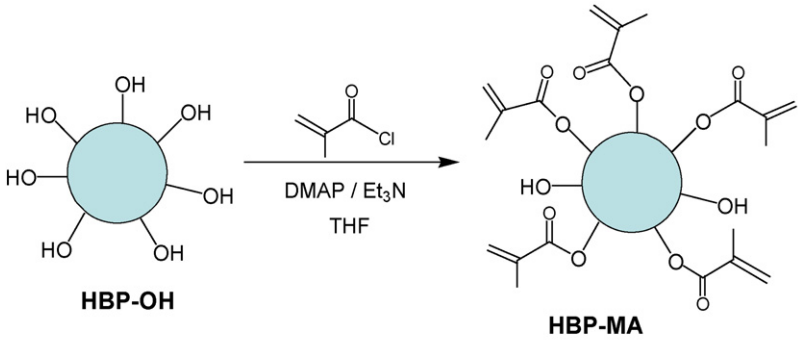

Scheme 2. Modification of hydroxyl end-groups of HBP to obtain methacrylic end-capped hyperbranched macromonomers.

peak is attributed to the gel effect for the bulk material when the resin was homogeneous, while the second one was due to the autoacceleration in the microgels. It is assumed that the reactivity of pendant double bonds is lower than that of the free unreacted monomer. As a result, the concentration of pendant groups increases during the polymerization reaction as the concentration of double bonds of free monomer is depleted. When the concentration of pendant vinyl groups is high they begin to react giving rise to microgel formation (local dense crosslinking) and a second autoacceleration in the reaction rate. Many of the unreacted pendant double bonds become entrapped in the microgel regions and their apparent reactivity decreases due to steric hindrance (thermodynamic excluded volume effect) [25]. Further reaction (macrogelation) occurs by the chemical bonding of microgel particles [26]. The formation of microgels is the reason for network inhomogeneity and this can lead to a significant reduction of the mechanical strength of the material.

Table 3 collects the data of the polymerization rate at 5% conversion (R_{pi}), the time at maximum rate of polymerization (t_{max}), the double bond conversion at the maximum polymerization rate (α_{tmax}) and final conversion (α_F) of the photopolymerization reaction using P1000MA as crosslinking agent.

The general trend is that polymerization rate increases slightly when monofunctional methacrylic monomers are photopolymerized in the presence of different amounts (between 2 and 8%, w/w) of P1000MA, with the exception of LMA. It is well known that π–π stacking between aromatic rings increases molecular rigidity [27] and may account for the increased reactivity of the system. The

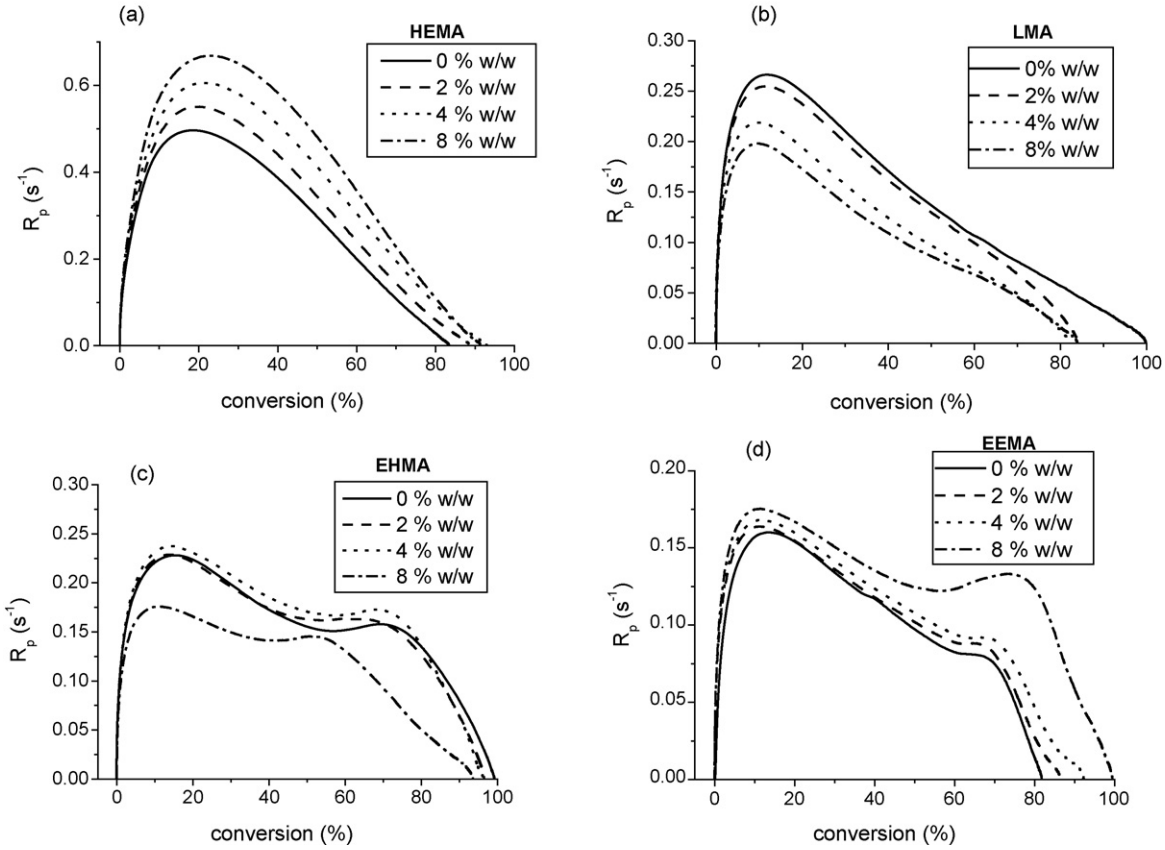

Fig. 4. Plots of polymerization rate as a function of conversion for several monomers in the presence of hyperbranched macromer P1000MA. (a) HEMA, (b) LMA, (c) EHMA and (d) EEMA.

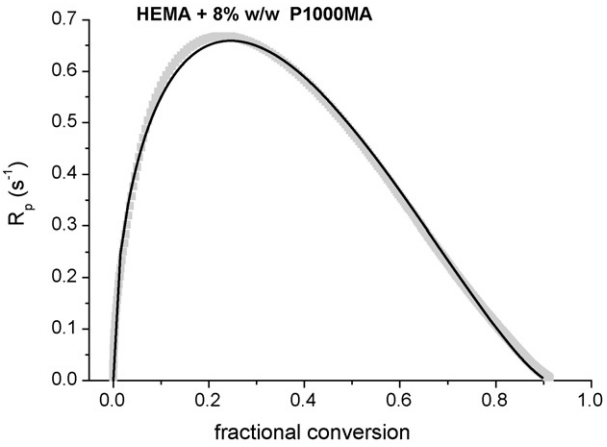

Fig. 5. Comparison of modified autocatalytic model (solid line) and the experimental data (gray box) for the UV-curing of HEMA in presence of hyperbranched macromer P1000MA (8%, w/w).

Table 2
Kinetic parameters of second order autocatalytic model for photopolymerization of HEMA in the presence of several amounts of P1000MA

P1000MA (%, w/w)	k (s^{-1})	m	n	r^2
0	1.95 ± 0.01	0.476 ± 0.006	1.452 ± 0.005	0.998
2	1.96 ± 0.02	0.471 ± 0.004	1.422 ± 0.008	0.995
4	2.01 ± 0.02	0.478 ± 0.004	1.366 ± 0.007	0.995
8	2.33 ± 0.02	0.500 ± 0.003	1.359 ± 0.005	0.998

time to reach the maximum polymerization rate increases with P1000MA concentration for LMA whereas it decreases for the rest of monomers. In the case of HEMA the reactivity increases abruptly with the increase of P1000MA concentration, exhibiting a twofold higher polymerization rate with 8% (w/w) of the multifunctional hyperbranched crosslinker. Comparing the kinetics of EEMA and HEMA, which have similar structure but differ only in the presence of a hydrogen-bond donor, the enhanced reactivity of the hydroxyl-terminated monomer could be explained due to hydrogen-bonding effects. Hydrogen-bonding increases the relative viscosity of the system, particularly during the early stage of polymerization. Intermolecular hydrogen bonds leads to a viscosity increase that results in reduced termination and enhanced polymerization kinetics [28].

In general, the extent of conventional photopolymerization reactions is affected by the presence of multifunctional monomers and lead to a decrease of the final conversion. This expected trend is only observed for the UV-curing of LMA and EHMA in the presence of P1000MA, whereas the final conversion increases with HBMm concentration for BMA, EEMA and HEMA (Fig. 6). The last feature is explained by the enhanced mobility of the system during photopolymerization. This hypothesis was confirmed by measuring the swelling ratio (Table 4). The swelling ratio of the photopolymerized BMA and HEMA films increases with P1000MA concentration.

Even though the high acrylic functionality of HBMm, the resins in its presence have lower unsaturation concentration due to their higher molecular weight in comparison to the monofunctional monomers. This dilution effect of double bond concentration may delay the gel point. Therefore, it is plausible that in these systems increasing HBMm content enhances the mobility, while providing more accessible space for the polymerization of acrylate to occur. This is in accordance with fluorescence results shown also in Table 3 and explained below. As a consequence of the dilution effect of double bond concentration by increasing the amount of HBMm in the formulation, the rigidity of the network diminishes, vitrification occurs at higher degrees of conversion and the limiting conversion increases. This fact seems to indicate that the accessibility to the reactive sites, as well as the double bonds, depends on topological factors, at least in the last stages of the photopolymerization reaction.

The kinetics of polymerization was also investigated in the presence of an aliphatic polyester hyperbranched macromer H30MA with an average of 16 methacrylic end-groups (from a total of 32 hydroxyl functionalities). The kinetic data are listed in Table 5. In all the cases, the monomer reactivity is enhanced in the presence of this hyperbranched polyester, showing higher polymerization rate as H30MA concentration increases for the studied monomers (HEMA, LMA, OMA and EEMA). The final conversion increases for

Table 3
Polymerization rate at 5% conversion (R_{pi}); time at the maximum rate of polymerization (t_{max}), double bond conversion at the maximum (α_{tmax}) and final conversion (α_{final}) of the photopolymerization reactions using P1000MA as crosslinking agent (kinetic parameters as t_{gel} and α_{tgel} were determined by fluorescence.)

Monomer	P1000MA (%, w/w)	R_{pi} (s^{-1})	α_F (%)	t_{max} (s)	α_{tmax} (%)	t_{gel} (s)	α_{tgel} (%)
HEMA	0	0.18	84	64	19	205	64
	2	0.23	88	65	20	277	77
	4	0.26	93	60	22	268	81
	8	0.30	91	57	23	221	80
LMA	0	0.20	100	67	12	–	–
	2	0.20	84	70	12	270	49
	4	0.17	82	73	10	235	38
	8	0.17	84	70	10	200	31
BMA	0	0.08	47	130	9	234(754)	18(41)
	2	0.12	49	106	11	195(702)	17(46)
	4	0.11	52	105	10	182(650)	20(54)
	8	0.12	67	102(928)	9(60)	182(923)	18(67)
EHMA	0	0.13	99	98(409)	15(50)	–	–
	2	0.15	97	87(363)	14(70)	182	34
	4	0.16	96	89(373)	14(68)	146	27
	8	0.13	94	83(346)	11(68)	130(793)	19(86)
EEMA	0	0.11	82	120(564)	14(64)	325	42
	2	0.12	86	98(549)	11(64)	234(663)	32(74)
	4	0.12	92	98(546)	12(67)	208(702)	29(79)
	8	0.14	100	91(537)	11(74)	117(728)	16(92)

For the kinetic profiles that showed multiple peaks, the data of second peak is given in parenthesis.

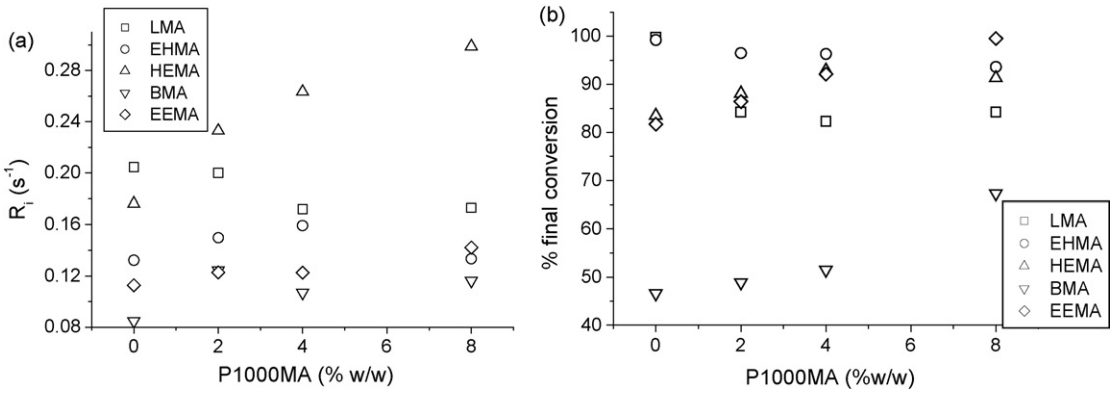

Fig. 6. Polymerization rate (a) and final conversion (b) as a function of the amount of P1000MA for the photopolymerization of several monofunctional monomers.

Table 4
Swelling ratio of methacrylic films photocrosslinked with hyperbranched P1000MA

Monomer	H30MA (%, w/w)	Swelling ratio	α_F (%)
HEMA	0	2.41 ± 0.08	84
	2	1.75 ± 0.02	88
	4	2.28 ± 0.02	93
	8	2.75 ± 0.08	91
BMA	0	1.43 ± 0.03	47
	2	2.12 ± 0.13	49
	8	2.79 ± 0.12	67

HEMA, OMA and EEMA and decreases slightly for LMA as H30MA increases. It seems to indicate that the functional end-groups of the H30MA are highly accessible for polymerization.

The copolymerization of difunctional monomers with H30MA was also investigated (Table 6). Both polymerization rate and conversion increase with H30MA concentration during its copolymerization with HDDMA due to the dilution effect of reactive double bonds. In the reaction with PEGDMA, the higher length of the spacer between the two methacrylic groups enables to obtain higher limiting conversion than with HDDMA. This late feature is attributed to the lower termination rate as a consequence of the lower rigidity of the network. In this case, the final conversion decreases as H30MA concentration increases.

Table 6
Polymerization rate at 5% conversion (R_{pi}); time at the maximum rate of polymerization (t_{max}), double bond conversion at the maximum (α_{tmax}) and final conversion (α_{final}) of the photopolymerization reaction of difunctional monomers using H30MA as crosslinking agent (kinetic parameters as t_{gel} and α_{tgel} were determined by fluorescence.)

Monomer	H30MA (%, w/w)	R_{pi} (s^{-1})	α_F (%)	t_{max} (s)	α_{tmax} (%)	t_{gel} (s)	α_{tgel} (%)
HDDMA	0	0.43	55	48	14	195	45
	2	0.52	59	47	14	221	55
	4	0.61	62	44	15	364	62
	8	0.64	68	45	17	390	68
PEGDMA	0	0.96	98	30	16	–	–
	2	0.95	92	29	13	312	91
	4	0.99	91	28	18	286	91
	8	1.01	86	29	19	234	85

The influence of the nature and the unsaturation degree of the hyperbranched macromers were analyzed by comparing photopolymerization kinetics of several methacrylic monomers in presence of a fixed amount of different HBMm (8%, w/w). Apart from the hyperbranched polyester H30MA, the three poly(ester-amide)s were studied (Table 7). Fig. 7 plots polymerization rates versus conversion for UV-curing of (a) LMA and (b) EEMA in the presence of 8% (w/w) of several hyperbranched macromers. The early stage of photopolymerization does not change very much by the presence of HBMm, in contrast, the appearance of

Table 5
Polymerization rate at 5% conversion (R_{pi}); time at the maximum rate of polymerization (t_{max}), double bond conversion at the maximum (α_{tmax}) and final conversion (α_{final}) of the photopolymerization reaction using H30MA as crosslinking agent (kinetic parameters as t_{gel} and α_{tgel} were determined by fluorescence.)

Monomer	HBMm (%, w/w)	R_{pi} (s^{-1})	α_F (%)	t_{max} (s)	α_{tmax} (%)	t_{gel} (s)	α_{tgel} (%)
HEMA	0	0.18	84	63	18	205	64
	2	0.27	98	60	24	210	84
	4	0.30	99	56	25	128	74
	8	0.33	98	52	21	–	–
OMA	0	0.19	76	106	17	169	31
	2	0.21	88	102	16	143(364)	25(72)
	4	0.18	98	118	18	208(507)	37(84)
	8	0.22	97	79(275)	15(63)	117(403)	24(87)
LMA	0	0.20	100	67	12	–	–
	2	0.24	98	69	12	442	74
	4	0.28	97	65	13	160(585)	39(93)
	8	0.28	95	66	13	184(676)	44(91)
EEMA	0	0.11	82	120(564)	14(64)	325	42
	2	0.13	82	97(532)	14(66)	328(720)	47(70)
	4	0.14	88	83(426)	11(61)	170(560)	24(79)
	8	0.13	98	94(397)	11(61)	105(520)	13(83)
	20	0.21	100	99(195)	21(53)	–	–

For the kinetic profiles that showed multiple peaks, the data of second peak is given in parenthesis.

Table 7
Comparison of kinetic parameters of the photopolymerization reaction of several monomers using a fixed amount (8%, w/w) of different HBMm as crosslinking agents

Monomer	HBMm	R_{pi} (s^{-1})	α_F (%)	t_{max} (s)	α_{tmax} (%)	t_{gel} (s)	α_{tgel} (%)
EHMA	–	0.13	99	99(409)	15(69)	–	–
	P1000MA	0.13	94	83(346)	11(68)	130(793)	19(86)
	D2000MA	0.18	98	87(269)	16(59)	234(661)	50(97)
	H30MA	0.19	96	90(352)	16(67)	247	48
	H1500MA	0.19	97	80(363)	14(72)	169(507)	35(94)
EEMA	–	0.11	82	120(564)	14(64)	325	42
	P1000MA	0.14	100	91(537)	11(74)	117(728)	16(92)
	D2000MA	0.13	95	94(397)	11(59)	170	23
	H30MA	0.13	98	94(397)	11(61)	105(520)	13(83)
	H1500MA	0.14	98	97(437)	12(67)	241	36
LMA	–	0.21	100	67	12	–	–
	P1000MA	0.17	84	70	10	200	31
	D2000MA	0.18	92	86	15	181	38
	H30MA	0.28	95	66	13	184	44
	H1500MA	0.22	92	71	13	129	28

For the kinetic profiles that showed multiple peaks, the data of second peak is given in parenthesis.

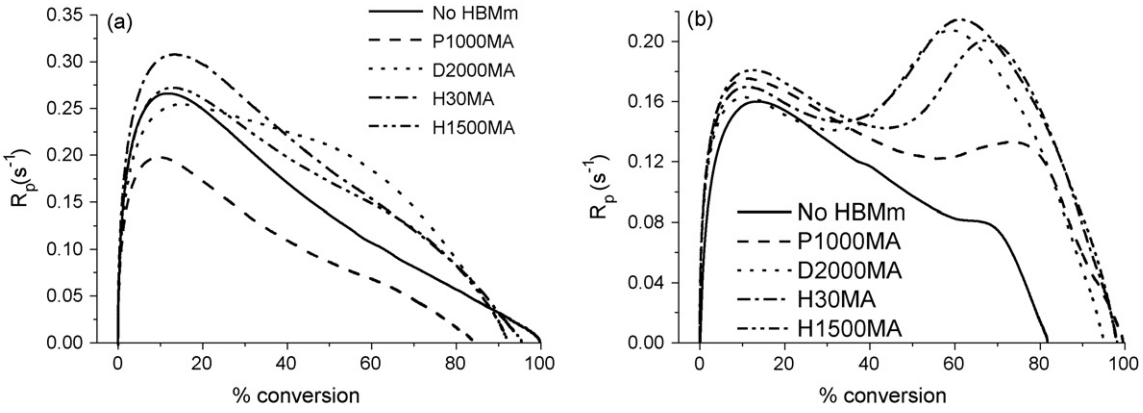

Fig. 7. Polymerization rate versus conversion for UV-curing of (a) LMA and (b) EEMA in the presence of 8% (w/w) of several hyperbranched macromers.

the second peak in the DSC profiles strongly depends on HBMm nature.

For a better understanding of the effect of the HBMm on photopolymerization kinetics of methacrylic monomers polymerization rate and final conversion are plotted as a function of the number of reactive groups in the HBMm (Fig. 8). The extent of the polymerization is reduced in the presence of HBMm for LMA and EHMA, whereas the final conversion increases for the copolymer-

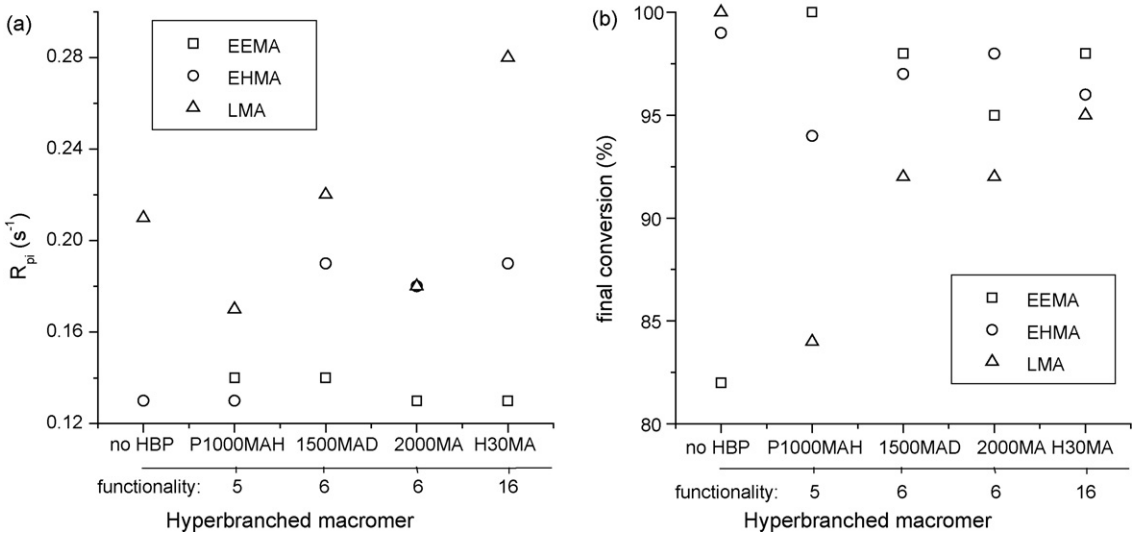

Fig. 8. Polymerization rate (a) and final conversion (b) as a function of the HBMm (at a fixed amount of 8%, w/w) for the photopolymerization of several monofunctional monomers. The abscissa axis shows the functionality referred as the average number of acrylic groups in the periphery of the modified HBMm.

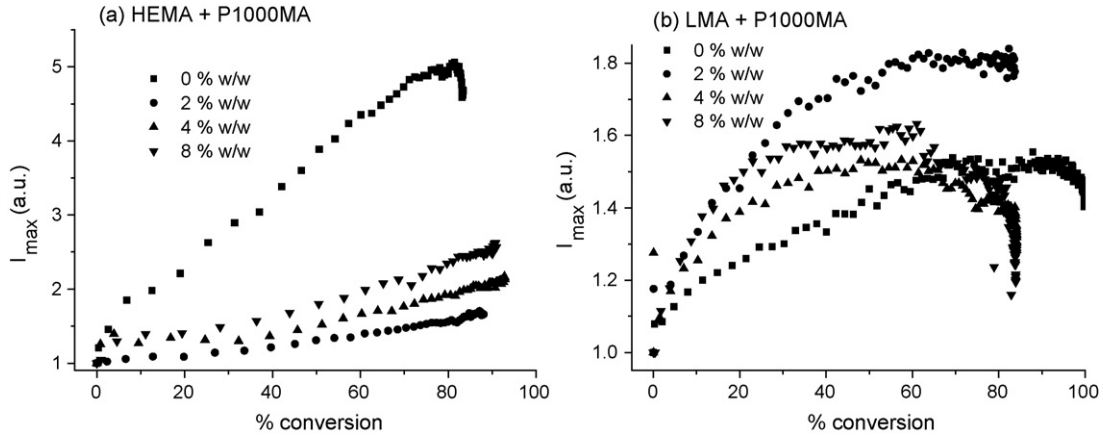

Fig. 9. Plot of the fluorescence intensity at maximum versus conversion for the photopolymerization of (a) HEMA and (b) LMA in the presence of different amounts of P1000MA.

ization of EEMA and any HBMm. In the experimental conditions the final conversion of EEMA photopolymerization is 82% and reaches 95–100% of conversion depending on the HBMm. However, the rate of the reaction does not scale simply with the number of acrylic functionalities of the HBMm which is attributed to diffusion limitations during the polymerization. Other authors [7] found that the combination of viscosity and concentration of unsaturation provides the clear evidence that polymerization rates in UV-curable waterborne hyperbranched polymers are not simply predictable.

3.3. Fluorescence monitoring

The fluorescent probe, derivative of styryl diazine (DMA-2,5), was used for monitoring photopolymerization. Previously, it was verified that the effect of probe concentration or probe presence/absence had no influence on the polymerization rate. Fluorescence spectra were recorded during irradiation time. The fluorimeter coupled to a DSC allows measuring a complete spectrum every 14 s. The home-built device provides confidence and reproducibility to correlate conversion and fluorescence changes during photopolymerization of acrylic monomers doped with fluorescent probes.

The fluorescence intensity of DMA-2,5 increases as photopolymerization/crosslinking proceeds using HBMm as crosslinker agents. This behaviour has been also observed during photopolymerization of mono- and difunctional monomers in bulk using this fluorescent probe, being useful for monitoring photopolymerization in homogenous and heterogeneous systems [16]. Fluorescent probes are sensitive to changes in the local rigidity of the medium. In a medium in which molecular mobility is restricted, fluorescence emission increases due to the associated restriction in the non-radiative relaxation pathway of the excited state of the probe. This non-radiative process normally involves some kind of vibrational coupling between the excited state and the environment.

Fig. 9 shows the fluorescence intensity at the maximum as a function of conversion for HEMA and LMA in the presence of different concentrations of P1000MA. The fluorescence intensity at the initial reaction time was used as an internal standard to calibrate any fluctuation during the curing process and from different experiments. The incorporation of the HBMm reduces the rigidity of the medium during the photopolymerization process resulting in a decrease of fluorescence intensity in the HEMA photopolymerization. This may be attributed to the disruption of hydrogen bonds by the addition of P1000MA enhancing the accessibility to acrylic moieties. This feature explains that the degree of conversion increased with P1000MA concentration, as shown in Table 3. Moreover, the increase of fluorescence with conversion followed a linear kinetics during the whole course of the reaction. Similar behaviour was observed for HEMA formulations containing H30MA or H1500MA. Fig. 9(b) shows that the fluorescence intensity at the maximum wavelength exhibits a higher increase during the photopolymerization of LMA for the formulations containing P1000MA or H30MA compared to that in the absence of crosslinker. This feature indicates a higher rigidity in the local environment of the probe in the presence of HBMm and therefore, a more restricted mobility of radicals leading to a polymer network that contains a higher residual amount of insaturations and trapped radicals. This is also confirmed by the DSC kinetics profile which showed that the reached conversion at the maximum polymerization rate slightly decreases with HBMm concentration increases (Table 3).

Moreover, all the data fall on a single smooth curve whose slope is much sharper at the initial stage of cure where fluorescence increases steadily with conversion and then, the fluorescence intensity becomes less sensitive to the photopolymerization process. The intersection point between the two slopes in the fluorescence curves has been associated to the gelation point [29]. Two kinetic parameters were determined from fluorescence profiles: t_{gel} and α_{tgel}, which are compiled in Tables 3 and 5–7 for the series of UV-curing reactions studied here. As HBMm concentration increases the gelation occurs at lower conversion and then, final conversion decreases for LMA and EHMA in the presence of P1000MA in our experimental conditions (Table 3). Whereas the conversion α_{tgel} increases with HBMm concentration for the formulations which reached higher final conversion as HBMm concentration also increases (i.e., HEMA, BMA and EEMA in the presence of P1000MA). Fig. 10 shows a good correlation between the final conversion determined by photoDSC and the conversion reached at gelation determined by fluorescence. Such results suggest that when a system is diluted, the enhanced intramolecular cyclization consumed so many pendant groups that gelation is delayed (or even prevented), as recently pointed out by Matyajaszewski for the synthesis of polyacrylate networks [30]. The extent of intramolecular cyclization compared to intermolecular crosslinking reaction depends on the concentration of the reagents in the system, as well as the chemical structures of monomers and crosslinkers, as inferred from the values of α_{tgel} in Table 7.

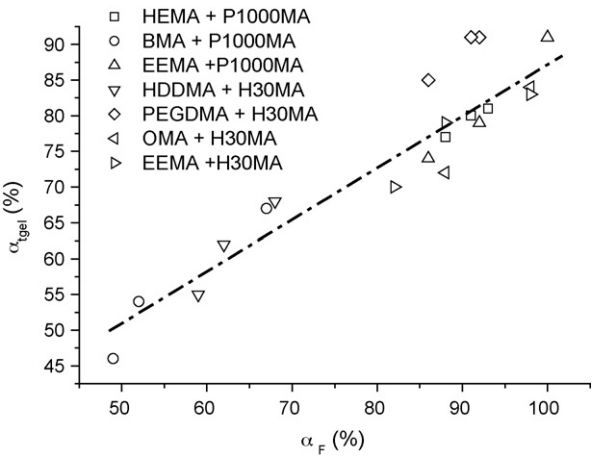

Fig. 10. Plot of α_{tgel} as a function of α_F for the UV-curing of several monofunctional monomers in the presence of P1000MA and difunctional monomers in the presence of H30MA.

The fluorescence intensity at the maximum wavelength versus degree of conversion for EEMA photopolymerization in the presence of P1000MA shows a more complex behaviour (Fig. 11). Three regions are distinguished with different slopes. The initial stage reveals a steep change of fluorescence intensity whereas a steady increase is observed after 10–20% of conversion is attained. A third region is observed only in the presence of P1000MA and an abrupt increase of the fluorescence intensity is detected as conversion increases. This behaviour seems to correlate with the expected changes of microviscosity during microgel formation followed by an abrupt increase due to the macrogelation by reaction between different microgel domains. During polymerization, fluorescence intensity for a given value of conversion depends on HBMm concentration. This confirms that crosslinking density does not develop equivalently as a function of conversion and agrees well with the kinetic features measured by DSC. Fig. 11(b) shows the ratio between the intensities at two wavelengths as a function of degree of conversion for this series of UV-curing reactions. The fluorescence increases abruptly with conversion in the last stage of EEMA photocuring in presence of P1000MA or H30MA at the same conversion that a second peak corresponding to microgel autoacceleration was monitored by DSC. Fluorescence monitoring provides additional insight into the changing morphology of this complex system and are in accordance with the proposed hypothesis of spatial heterogeneity.

Fluorescence monitoring of photopolymerization of difunctional monomers confirmed that the role of HBMm is dependent on the nature of the reactive monomer. In the case of HDDMA photopolymerization, H30MA acts as a reactive diluent decreasing the viscosity of the media (fluorescence intensity decreases as H30MA concentration increases) and thus, leading to a higher final conversion. However, during PEGDMA photopolymerization, fluorescence increases more rapidly in the presence of H30MA than in its absence and gives rise to a slight decrease of final conversion as H30MA concentration increases. Also a good correlation

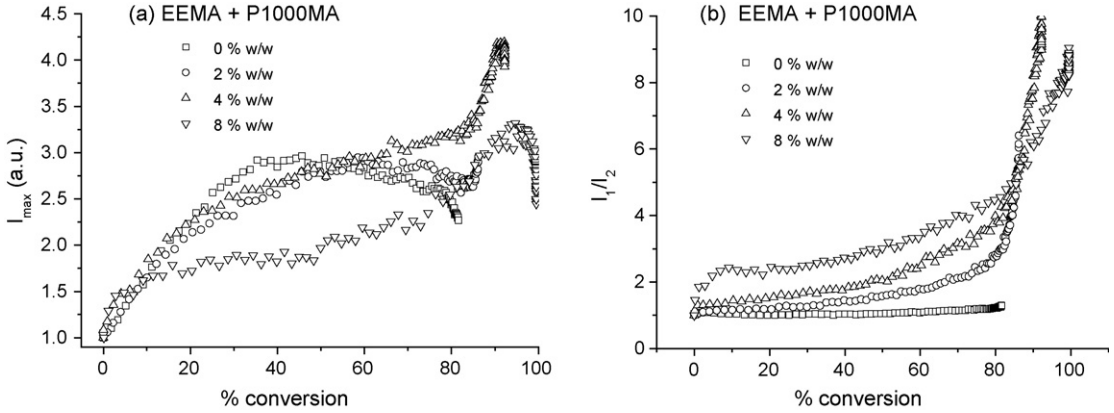

Fig. 11. Comparison of the plots of (a) fluorescence intensity at maximum versus conversion and (b) ratio of intensities at two wavelength versus conversion for the photopolymerization of EEMA in the presence of different amounts of P1000MA.

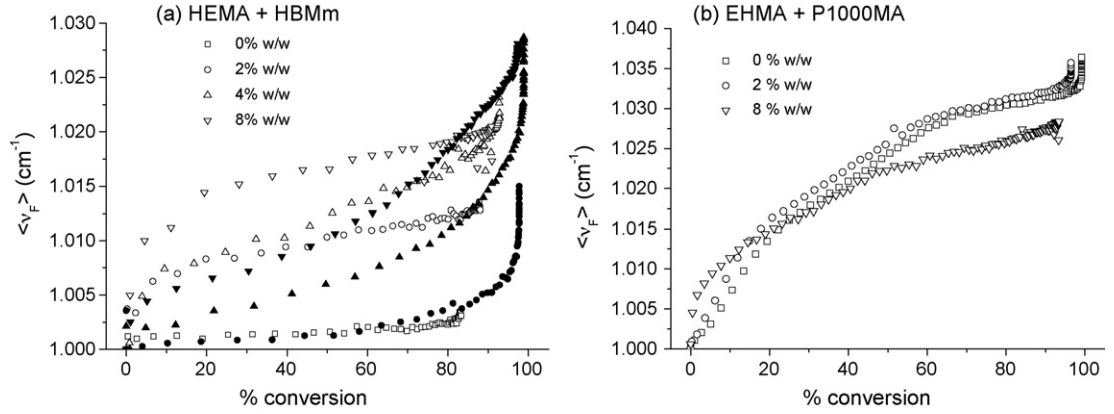

Fig. 12. Changes of the first moment of fluorescence as a function of conversion for the photopolymerization of (a) HEMA and (b) EHMA in the presence of different amounts of HBMm. Solid symbols: H30MA and open symbols: P1000MA.

is found between fluorescence and photoDSC results as shown in Fig. 10.

In Fig. 12 the first moment of fluorescence, $\langle \nu_F \rangle$, is plotted as a function of conversion for the polymerization of HEMA and EHMA in the presence of HBMm. The mathematical treatment of the experimental data (emission spectra between 400 and 560 nm) for calculation of the first moment has led to an accurate correlation between fluorescence and degree of conversion with a lower scatter of data compared to the plots of fluorescence intensity as a function of conversion. Also, it shows high sensitivity at the range of high conversion which is of great interest from an applied viewpoint although monitoring of UV-curing reaction by following the $\langle \nu_F \rangle$ changes seems to be less sensitive for polar monomers than that for non-polar monomers.

The origin of the changes in the emission spectra is rather complex. In solvatochromic probes with a strong dipole moment in the excited state the typical behaviour during a curing reaction consists of shifting the average emission energy towards higher energies due to an increasingly inefficient coupling between the excited state dipole and the environment. In this regard, the first moment of fluorescence practically does not change as HEMA photopolymerization occurs as result of the high polarity of the medium. However, the incorporation of P1000MA brings about an abrupt increase of the $\langle \nu_F \rangle$ when less than 20% of conversion was reached. This behaviour is explained by a decrease of polarity which is dependent on P1000MA feed. Here, we propose that P1000MA may cause the disruption of intermolecular hydrogen bonds between HEMA molecules, for example due to P1000MA self-assembling by π-stacking. Therefore, the presence of P1000MA aggregates favours a large decoupling of excited dipole moment and the environment. However, the change of the $\langle \nu_F \rangle$ with conversion depends slightly on P1000MA feed during EHMA photopolymerization. This last monomer, as commented earlier, posses a similar structure than HEMA without the chance to form hydrogen bonds. Therefore, the increasingly inefficient coupling of probe excited state with the medium is attributed to the decrease of polarity as vinyl groups disappear during the course of the reaction together with the increasing rigidity of the medium.

Using H30MA as crosslinker of HEMA the increase of the $\langle \nu_F \rangle$ with conversion is lower than using P1000MA (Fig. 12a). This may be due to the higher polarity of H30MA which posses about 14–16 hydroxyl groups in its periphery (the rest of 32 moieties are methacrylic end-groups) compared to P1000MA which has an average of 3 hydroxyl and 5 methacrylic end-functionalities.

3.4. Morphology and thermal characterization

Most of the films obtained after UV-curing were transparent. However, the copolymerization of P1000MA with EHMA and LMA as well as H30MA with EHMA resulted in translucent films. This is in accordance with the spatial heterogeneity induced in these films by microgel formation.

Thermal stability was analyzed by thermogravimetric measurements. Fig. 13 shows TGA curves for selected networks. The general trend is an increase of the onset degradation temperature with HPBMm in the photopolymerized films. The increases of degradation temperature may be attributed to a higher heterogeneous rigid region. For example, for HEMA (onset point = 244 °C) an increase between 90 and 100 °C is observed depending on the concentration and nature of the hyperbranched macromer. For comparison the TGA curves of the samples photocured with HBMm, D2000MA and H30MA, are included in the figure and show a more rapid degradation processes starting at lower temperatures. The highest thermal

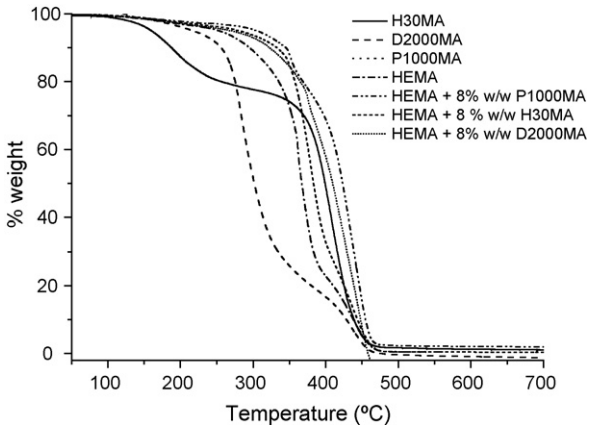

Fig. 13. TGA curves for selected networks of photopolymerized HPBMm and HEMA in the presence of 8% (w/w) of HBMm. The hyperbranched macromers were P1000MA, D2000MA and H30MA.

stability corresponded to the materials containing P1000MA as a result of the aromatic rings incorporated in the structure of the networks. Table 8 shows the TG parameters for the series of HEMA and EEMA obtained from the derivative of TG curves. The degradation process is illustrated by the onset and the maximum temperature peak of the first degradation step, T_{1max}, along with the same for the second step, T_{2max}. While the second peak becomes more pronounced with P1000MA/H30MA content for HEMA-based networks, T_{2max} remains practically invariable. An opposite trend was observed for EEMA. The second peak becomes less pronounced as H30MA content increases and T_{2max} is shifted to lower temperatures, indicating phase mixing. For each series, increasing the content of HBMm the TG curves shift to higher temperatures. This implies that the use of HBMm may improve the thermal stability of acrylic-based coatings.

DSC results show similar T_g for HEMA networks prepared in presence of P1000 or H30, However, the glass transition temperature of networks decreases to around 60 °C in comparison with the pure HEMA (T_g = 64 °C). In spite of morphologies show differences depending on HBMm feed, no significant deviation from the pure component value for T_g exhibited by the networks. P1000MA has T_g at 95 °C and H30MA at 35 °C, in the networks the T_{gs} could not be discernible by DSC.

SEM micrographs of cryogenic fracture of HEMA photopolymerized films are shown in Fig. 14. The cross-sectional morphologies of crosslinked HEMA networks with different amount of crosslinker H30MA are combined together for comparison. The specimens of pristine HEMA films are characterized by minor surface het-

Table 8
TGA parameters: the onset and the maximum temperature peak of the first degradation step, $T_{1max,}$ along with the same for the second step, T_{2max}, and temperature of degradation, T_d, as the temperature at 5 % weight loss

Monomer	HBMm	% (w/w) of HBMm	T_{on} (°C)	T_{1max} (°C)	T_{2max} (°C)	T_d (°C)
HEMA	–	0	245	363	437	253
	P1000MA	2	334	361	435	274
	P1000MA	8	339	358	430	291
	H30MA	2	347	374	443	280
	H30MA	4	313	375	434	270
	H30MA	8	348	379	434	280
EEMA	–	0	154	305	383	182
	H30MA	2	187	287	374	203
	H30MA	4	258	296	359	229
	H30MA	8	197	298	349	196

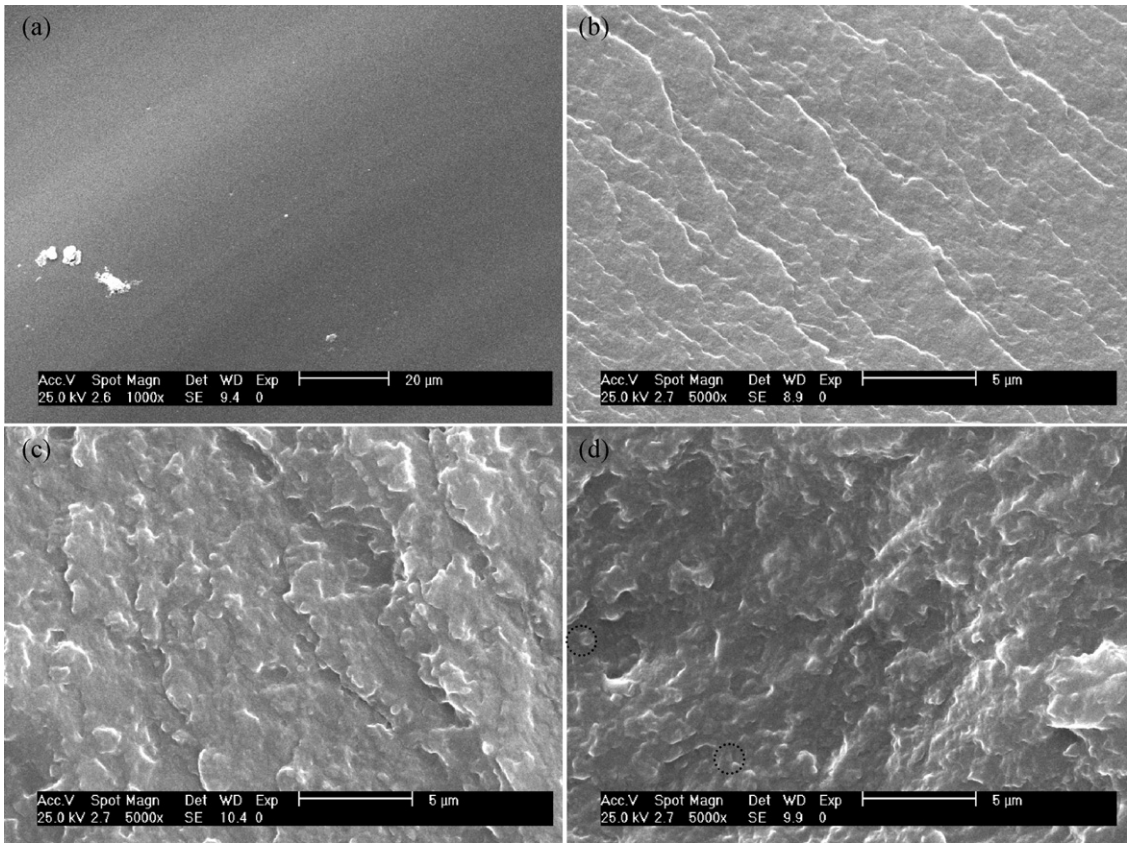

Fig. 14. SEM micrographs of cryogenic fracture of photopolymerized films of HEMA in presence of different amounts of H30MA.

erogeneities and a dense bulk phase (Fig. 14a), which is typical in brittle fracture. Spherulite-like domains with a size less than 1 μm were observed in the surface (micrographs not shown). The cross-sectional micrograph shows a bulk phase. In contrast, the fracture surfaces of HEMA-based networks are rather more coarse and rougher as concentration of H30MA increases, as shown in Fig. 14b–d, suggesting that the specimens break more yielding than that of pure HEMA. In other words, it is expected an increase of impact stress by the addition of UV-curable HBMm. As can be seen from Fig. 14d, the cured H30MA particles are enwrapped tightly by the HEMA matrix. The crosslinking reaction between HEMA and H30MA contributes to a certain degree of improvement in the interfacial adhesion between the matrix and particles.

After cryogenic fracture SEM micrographs show holes in some specimens (see Fig. 15). At the highest used concentration of hyperbranched monomer, phase separation may occur resulting in a dispersed particulate/holes structure. Reaction induced phase separation is favoured in the systems which have shown a delay in the gel point as concentration of HBMm increases. This may allows to obtain materials that retain the modulus at the same time that the toughness is increased by the introduction of small micron size separated particles into the acrylic network [31]. Phase separation may be induced by differences between the reaction kinetics of the HBMm and that of the methacrylic monomers. Moreover, the π–π^* stacking interactions between phenyl groups of P1000MA and H-bonds can drive the molecular self-assembly process to form clusters inside the acrylic matrix that strengthen the macroscopic structure. However, the toughening effect of these particles, whatever their nature and properties, depends on their size, interparticle distance, particle/matrix interaction and volume fraction and needs further investigation.

The mechanical properties will be further studied in detail, although some of these results are presented here in Table 9. Compression modulus was measured for films prepared by crosslinking HEMA with different amounts of P1000MA and H30MA, before and after swelling in ethanol. On one hand, the compression modulus increases as P1000MA feed for HEMA-based networks, accompanied by an increase of density. On the other hand, swelling ratio also increases with HBMm concentration. This last feature indicates a lower degree of crosslinking although density increases with P1000MA amount. Therefore, the enhancement of modulus and density with P1000MA feed amount may be explained inasmuch as phase separation and loss of free volume occurs. The modulus after swelling in ethanol decreases abruptly compared to non-swollen materials and also the lowest value of the modulus corresponds to the swollen network containing the highest concentration of P1000MA. It has been proposed that P1000MA self-assembles giving rise to aggregates that may be partially extracted during ethanol swelling leading holes that decrease compression modulus. Using H30MA as crosslinker the compression modulus after swelling also decreases for the highest concentration of HBMm, although the decrease is lower compared to that with P1000MA which may be attributed to the higher number of reactive end-groups in H30MA.

Self-assembly of hyperbranched polymers may account to change the physical properties during photocrosslinking of methacrylic-based networks. Besides the molecular structures, the self-assembly of hyperbranched polymers is affected by several factors such as the molecular concentration and nature of the monomer. In this paper, it is provided evidence that the gelation delay as HBMm concentration increases plays an important role to induce phase separation.

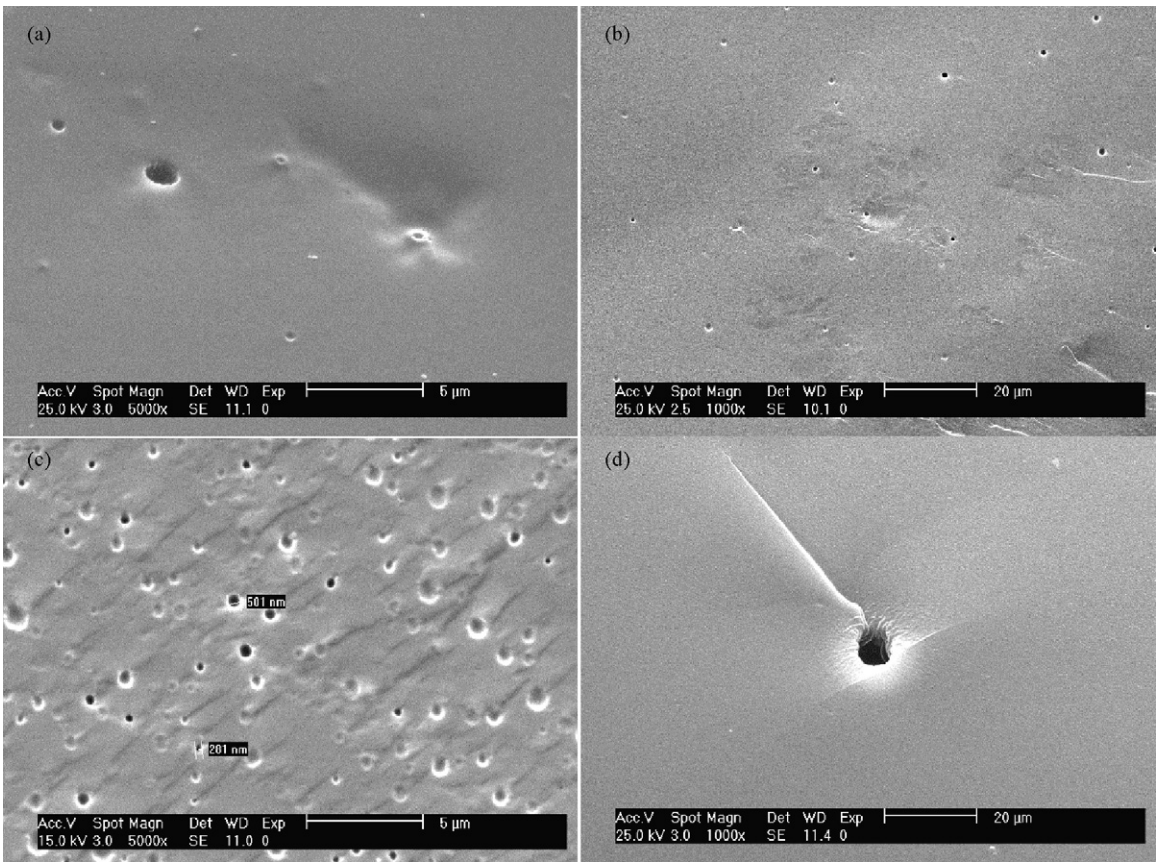

Fig. 15. SEM micrographs of cryogenic fracture of photopolymerized films of (a) HEMA + P1000MA, (b) BMA + P1000MA, (c) HEMA + D2000 and (d) OMA + H30MA. Concentration of HBMm was 8 wt.%.

Table 9
Compression modulus, density and swelling ratio of HEMA-based crosslinked networks

Crosslinker	HBP (%, w/w)	Swelling ratio	α_F (%)	Density (g/cm^3)	Modulus (10^{-6} Pa)	Modulus[a] (10^{-3} Pa)
P1000MA	0	2.41 ± 0.08	84	1.2593	278 ± 65	784 ± 75
	2	1.75 ± 0.02	88	1.2485	128 ± 31	912 ± 235
	4	2.28 ± 0.02	93	1.2671	153 ± 55	1059 ± 59
	8	2.75 ± 0.08	91	1.2757	210 ± 28	280 ± 5
H30MA	2	2.42 ± 0.03	98	1.2435	162 ± 23	896 ± 128
	4	2.77 ± 0.13	99	1.2496	285 ± 64	966 ± 36
	8	2.70 ± 0.12	98	1.2323	217 ± 33	551 ± 98

[a] Compression modulus after swelling in ethanol.

4. Conclusions

Fully cured networks were obtained by using hyperbranched macromers, HBMm, as crosslinker during UV-curing of mono- and difunctional methacrylic monomers. Multifunctional hyperbranched macromers copolymerize with methacrylic monomers allowing to overcome topological factors and vitrification that limit final conversion of conventional multifunctional monomers.

The incorporation of hyperbranched macromers to UV-curable methacrylic monomers causes an increase of the free volume fraction as confirmed by fluorescence. As HBMm concentration increases the gelation point is delayed and thus, results in an increase of final conversion. This behaviour is dependent on the concentration and the structures of the monomers and HBMm. A good correspondence has been found between gelation point, determined by fluorescence, and final conversion monitored by photoDSC. In particular, fluorescence monitoring of UV-curing enables to obtain information of the rigidity/microviscosity of the medium during the reaction and, an abrupt increase of fluorescence intensity and first moment has been measured corresponding to the microgel formation stage.

Finally, phase separation occurs at the highest used concentration of hyperbranched monomer, resulting in a dispersed particulate/holes structure. Self-assembly of methacrylic-modified hyperbranched polymers may favour the photopolymerization induced phase separation leading to materials with enhanced toughening characteristics.

Acknowledgements

The authors would like to thank the Plan Nacional I+D+I (Ministerio de Ciencia e Innovación) for financial support (MAT2006-05979) as well as the Comunidad Autónoma de Madrid for the funding through I+D Program (S0505/MAT-0227).

References

[1] N. Moszner, U. Salz, Prog. Polym. Sci. 26 (2001) 535–576.
[2] H. Kilambi, S.K. Reddy, L. Schneidewind, J.W. Stanbury, C.N. Bowman, Polymer 48 (2007) 2014–2021.
[3] H. Bergenudd, P. Eriksson, C.D. Armitt, B. Stenberg, E. Malmström, Polym. Deg. Stabil. 76 (2002) 503–509.
[4] E. Malmström, M. Trollsås, C.J. Hawker, M. Johansson, A. Hult, Adv. Polym. Sci. 143 (1999) 1.
[5] T.J. Mulkern, N.C. Beck Tan, Polymer 41 (2000) 3193–3203.
[6] A. Asif, C.Y. Huang, W.F. Shi, Colloid Polym. Sci. 283 (2005) 721–730.
[7] A. Asif, W. Shi, X. Shen, K. Nie, Polymer 46 (2005) 11066–11078.
[8] K. Maruyama, H. Kudo, T. Ikehara, T. Nishikubo, Macromolecules 40 (2007) 4895–4900.
[9] Q. Si, X. Wang, X. Fan, S. Wang, J. Polym. Sci. A: Polym. Chem. 43 (2005) 1883–1894.
[10] H. Kou, A. Asif, W. Shi, Eur. Polym. J. 38 (2002) 1931–1936.
[11] L. Boogh, B. Pettersson, J.E. Månson, Polymer 40 (1999) 2249–2261.
[12] G. Xu, W. Shi, M. Gong, F. Yu, J. Feng, Eur. Polym. J. 40 (2004) 483–491.
[13] G. Jannerfeldt, L. Boogh, J.-A.E. Månson, Polymer 41 (2000) 7627–7634.
[14] S. Peleshanko, V.V. Tsukruk, Prog. Polym. Sci. 33 (2008) 523–580.
[15] P. Bosch, F. Catalina, T. Corrales, C. Peinado, Chem. Eur. J. 11 (2005) 4314–4325.
[16] C. Peinado, P. Bosch, V. Martín, T. Corrales, J. Polym. Sci. A: Chem. 44 (2006) 5291–5303.
[17] C. Peinado, E.F. Salvador, A. Alonso, T. Corrales, J. Baselga, F. Catalina, J. Polym. Sci. A: Chem. 40 (2002) 4236–4244.
[18] P. Bosch, C. Peinado, V. Martín, F. Catalina, T. Corrales, J. Photochem. Photobiol., A: Chem. 180 (2006) 118–129.
[19] F. Mikes, J. González-Benito, J. Baselga, J. Macromol. Sci. Phys. B40 (2001) 405–428.
[20] J. Brandrup, E.H. Immergut, E.A. Grulke (Eds.), Polymer Handbook, 4th ed., John Wiley and Sons, 1999.
[21] E. Andrzejewska, Prog. Polym. Sci. 26 (2001) 605–665.
[22] M.R. Kamal, S. Sorour, Polym. Eng. Sci. 13 (1973) 59.
[23] J.H. Lee, J.W. Lee, Polym. Eng. Sci. 34 (1994) 9.
[24] K. Oiré, A. Otagawa, M. Muraoka, I. Mita, J. Polym. Sci., Polym. Chem. Ed. 13 (1975) 445–454.
[25] J.G. Kloosterboer, Adv. Polym. Sci. 84 (1988) 1–61.
[26] S. Ziaee, G.R. Palmase, J. Polym. Sci. Polym. Phys. 37 (1999) 725–744.
[27] H. Kilambi, J.W. Stanbury, C. Bowman, Macromolecules 40 (2007) 47–54.
[28] T.Y. Lee, T.M. Roper, E.S. Jonsson, C.A. Guymon, C.E. Hoyle, Macromolecules 37 (2004) 3659–3665.
[29] F. Mikes, J. González-Benito, J. Baselga, J. Polym. Sci. B: Polym. Phys. 42 (2004) 64–78.
[30] H. Gao, W. Li, K. Matyjaszwki, Macromolecules 41 (2007) 2335–2340.
[31] M. Johansson, T. Glausser, A. Jansson, A. Hule, E. Malmström, H. Claesson, Prog. Org. Coat. 48 (2007) 194–200.